Check for updates

OPEN

Human ZKSCAN3 and Drosophila M1BP are functionally homologous transcription factors in autophagy regulation

Marine Barthez[1], Mathilde Poplineau[2], Marwa Elrefaey[1], Nathalie Caruso[1], Yacine Graba[1] & Andrew J. Saurin[1] ✉

Autophagy is an essential cellular process that maintains homeostasis by recycling damaged organelles and nutrients during development and cellular stress. ZKSCAN3 is the sole identified master transcriptional repressor of autophagy in human cell lines. How ZKSCAN3 achieves autophagy repression at the mechanistic or organismal level however still remains to be elucidated. Furthermore, *Zkscan3* knockout mice display no discernable autophagy-related phenotypes, suggesting that there may be substantial differences in the regulation of autophagy between normal tissues and tumor cell lines. Here, we demonstrate that vertebrate ZKSCAN3 and Drosophila M1BP are functionally homologous transcription factors in autophagy repression. Expression of ZKSCAN3 in Drosophila prevents premature autophagy onset due to loss of M1BP function and conversely, M1BP expression in human cells can prevent starvation-induced autophagy due to loss of nuclear ZKSCAN3 function. In Drosophila ZKSCAN3 binds genome-wide to sequences targeted by M1BP and transcriptionally regulates the majority of M1BP-controlled genes, demonstrating the evolutionary conservation of the transcriptional repression of autophagy. This study thus allows the potential for transitioning the mechanisms, gene targets and plethora metabolic processes controlled by M1BP onto ZKSCAN3 and opens up Drosophila as a tool in studying the function of ZKSCAN3 in autophagy and tumourigenesis.

Macroautophagy (hereafter simply termed autophagy) is an evolutionary conserved process in eukaryotes by which protein aggregates and damaged organelles are degraded by the lysosome and is implicated in several central biological processes including tissue remodelling during development, starvation adaptation, anti-aging, tumour suppression, and cell death (reviewed in[1,2]). Given its importance in cellular homeostasis and development, defects in autophagy and its regulation have been associated with numerous diseases such as cancer, neuro-degenerative diseases (Parkinson) and diabetes (reviewed in[3–6]). Given the plethora pathophysiological processes linked to autophagy deregulation, it is not surprising that intense research has been directed into how normal autophagic processes are regulated.

The mammalian target of rapamycin (mTor) kinase is an important regulator of autophagy induction where active mTOR suppresses autophagy while inhibition of mTOR activity promotes autophagy onset[7], although a growing number of examples of mTOR-independent autophagy induction have been reported providing the notion that autophagy induction is not a single linear process but can rather be induced through the action of multiple interconnected key regulators[8]. While autophagy is largely a cytoplasmic event, recent studies have focussed on the nuclear transcription factors and epigenetic marks that modulate the expression of various auto-phagic components (reviewed in[9,10]). To date, more than 30 vertebrate transcription factors have been identified as positive transcriptional regulators of autophagy through activation of autophagy-related genes in vertebrates in response to various cellular stresses (reviewed in[11,12]). For example, under conditions of nutrient deprivation, phosphorylation of the MiTF transcription family member, TFEB by the mTor kinase in the cytoplasm results in its nuclear translocation and transcription of numerous autophagy-related genes[13], a process that is evolutionary conserved in Drosophila[14].

[1]Aix Marseille Université, CNRS, IBDM, UMR 7288, Marseille, 13288, Cedex 09, France. [2]Epigenetic Factors in Normal and Malignant Hematopoiesis, Aix Marseille Université, CNRS, INSERM, Institut Paoli-Calmettes, CRCM, Marseille, France. ✉e-mail: andrew.saurin@univ-amu.fr

1

While numerous transcription factors activating autophagy have been identified and extensively studied, comparatively few are known to be clear inhibitors of autophagy induction. Nonetheless, master transcriptional repressors of autophagy have been identified in vertebrates and Drosophila. In Drosophila, the Hox family of transcription factors have been described as master transcriptional repressors of autophagy induction, where the clearance of all Hox proteins is required for either starvation or developmental autophagy induction[15]. In vertebrates, the zinc finger with a SCAN and a KRAB domain 3 (ZKSCAN3) has been described as a master transcriptional repressor of autophagy[16], where its cytoplasmic relocation from the nucleus through JNK2-mediated phosphorylation is required for starvation or lysosomal stress-induced autophagy induction[17]. However, knockout mice lacking *Zkscan3* expression show no discernable phenotypes and no misexpression of components of the autophagic process, which would be expected from loss of a transcription repressor of autophagy[18]. The explanation given to explain this lack of autophagy phenotypes is that either the highly related *Zkscan4* gene could compensate for lack of Zkscan3 function or that outside of transformed cell line *in vitro* models, Zkscan3 in animal tissues is not a repressor of autophagy[18].

If the transcription factors driving autophagy activation are mostly conserved throughout evolution[14,19–21], it is less clear whether this is the case for transcription factors responsible for preventing autophagy induction. Given that the SCAN and KRAB domain are only found in vertebrate transcription factors, identifying a Drosophila homologue of ZKSCAN3 through similarity searches is not as straight forward as for other transcription factors. Nonetheless, Drosophila M1BP is a functional cofactor of Drosophila Hox proteins[22] and the presence of both M1BP and Hox are required for preventing autophagy induction in the Drosophila fat body[15,22]. Thus, while structural similarity between Drosophila M1BP and vertebrate ZKSCAN3 is restricted to their C-terminal C2H2 zinc finger domains, they are both required for autophagy inhibition. Moreover, the zinc finger associated domain (ZAD) of M1BP, while restricted to zinc finger proteins of dipteran and closely related insects, is analogous to the vertebrate KRAB domain, participating in a lineage-specific expansion of zinc finger proteins in insect and vertebrate genomes[23–25]. Together, these functional and structural similarities led us to hypothesise that Drosophila M1BP and vertebrate ZKSCAN3 are functionally homologous proteins.

Here, we show that expression of vertebrate ZKSCAN3, but not ZKSCAN4, in the Drosophila fat body prevents premature developmental autophagy induction caused by the loss of M1BP expression. Additionally, ZKSCAN3 binds the same genomic loci as M1BP in Drosophila cells and in the Drosophila fat body ZKSCAN3 transcriptionally controls two-thirds of M1BP-controlled genes. Similarly, we show that expression of M1BP in vertebrate cells is sufficient to prevent starvation-induced autophagy due to the cytoplasmic translocation of ZKSCAN3. Taken together, these data provide evidence that vertebrate ZKSCAN3 and Drosophila M1BP are functional homologues in the control of autophagy.

Results

ZKSCAN3 expression in the Drosophila fat body rescues premature autophagy induced by M1BP loss-of-function.

There are 23 vertebrate C2H2 zinc finger transcription factors containing SCAN and KRAB domains. Of these, ZKSCAN4 is the most similar to ZKSCAN3 in terms of sequence identity (Fig. 1A,B). It has been proposed that the high sequence identity between ZKSCAN3 and ZKSCAN4 may result in functional redundancy, which could explain the absence of autophagy-related phenotypes in ZKSCAN3-null mice[18]. As both ZKSCAN3 and ZKSCAN4 share similar levels of identity to M1BP (Fig. 1B), to study functional homology with Drosophila M1BP, we created independent myc-tagged ZKSCAN3 and ZKSCAN4 transgenic Drosophila fly lines under the expression control of the Gal4/UAS system[26]. Ubiquitous expression of either vertebrate gene using the ubiquitous Act5C-Gal4 driver had no apparent deleterious effects on general Drosophila health or longevity (Fig. 1C).

The Drosophila fat body, a nutrient storage organ analogous to the vertebrate liver, is commonly used to study autophagy since autophagy in the Drosophila fat body is engaged as both an essential developmental process required for metamorphosis to give rise to the adult fly[27,28] and in response to nutrient deprivation under starvation conditions[29]. When expressed in the Drosophila fat body using the cgGal4 driver, both ZKSCAN3 and ZKSCAN4 are expressed as full-length proteins (Fig. 1D) and, like in vertebrate cells[30], both are mainly nuclear (Fig. 1E), with weak accumulation observed in the cytoplasm (see Fig. S1) with no apparent effects on fat body size or developmental progression (data not shown).

In the third instar larval feeding stage (L3F), autophagy is blocked because of the action of M1BP and Hox proteins[15,22]. Loss of expression of M1BP through RNA interference (RNAi) rapidly induces autophagy in the L3F stage ([22] and see Fig. 2A). To test whether the co-expression of ZKSCAN3 or ZKSCAN4 is capable of preventing autophagy induction due to M1BP knockdown, we co-expressed either ZKSCAN3 or ZKSCAN4 with M1BP RNAi and monitored autophagy induction by cytoplasmic Atg8a accumulation, which is a marker of early autophagy induction, where its nuclear export into the cytoplasm is followed by lipidation recruiting it to early autophagosome membranes[31]. Whether ubiquitously expressed in the fat body using the cgGal4 driver (Fig. 2A) or by clonal analyses (Fig. 2B), we found that the expression of ZKSCAN3, but not ZKSCAN4, rescues M1BP RNAi-induced autophagy as observed by the absence of cytoplasmic Atg8a (Fig. 2A,B). While it has been suggested that ZKSCAN4 may be able to compensate for ZKSCAN3 in ZKSCAN3-mediated autophagy repression[18], these data demonstrate that in Drosophila at least, ZKSCAN4 cannot replace ZKSCAN3 in autophagy repression induced by loss of M1BP function. M1BP RNAi induces increased Atg8a expression (Atg8a-I) and lipidation of Atg8a (Atg8a-II), indicating increased autophagosome-associated Atg8a, and this is largely prevented upon ZKSCAN3 co-expression (Fig. 2C). ZKSCAN3 expression alone had no effect on nuclear localisation (Fig. S1A,B) and little effect on expression (see Fig. 2C) of Atg8a suggesting that the autophagy rescue observed by ZKSCAN3 is not simply due to ectopic repression of Atg8a expression levels in the non-autophagic cellular state. Like Atg8a, Atg8b and Atg7 are also essential for autophagosome formation[32–35]. Similarly to Atg8a, we observed that co-expression of ZKSCAN3 restores expression of these early autophagosome markers that are prematurely
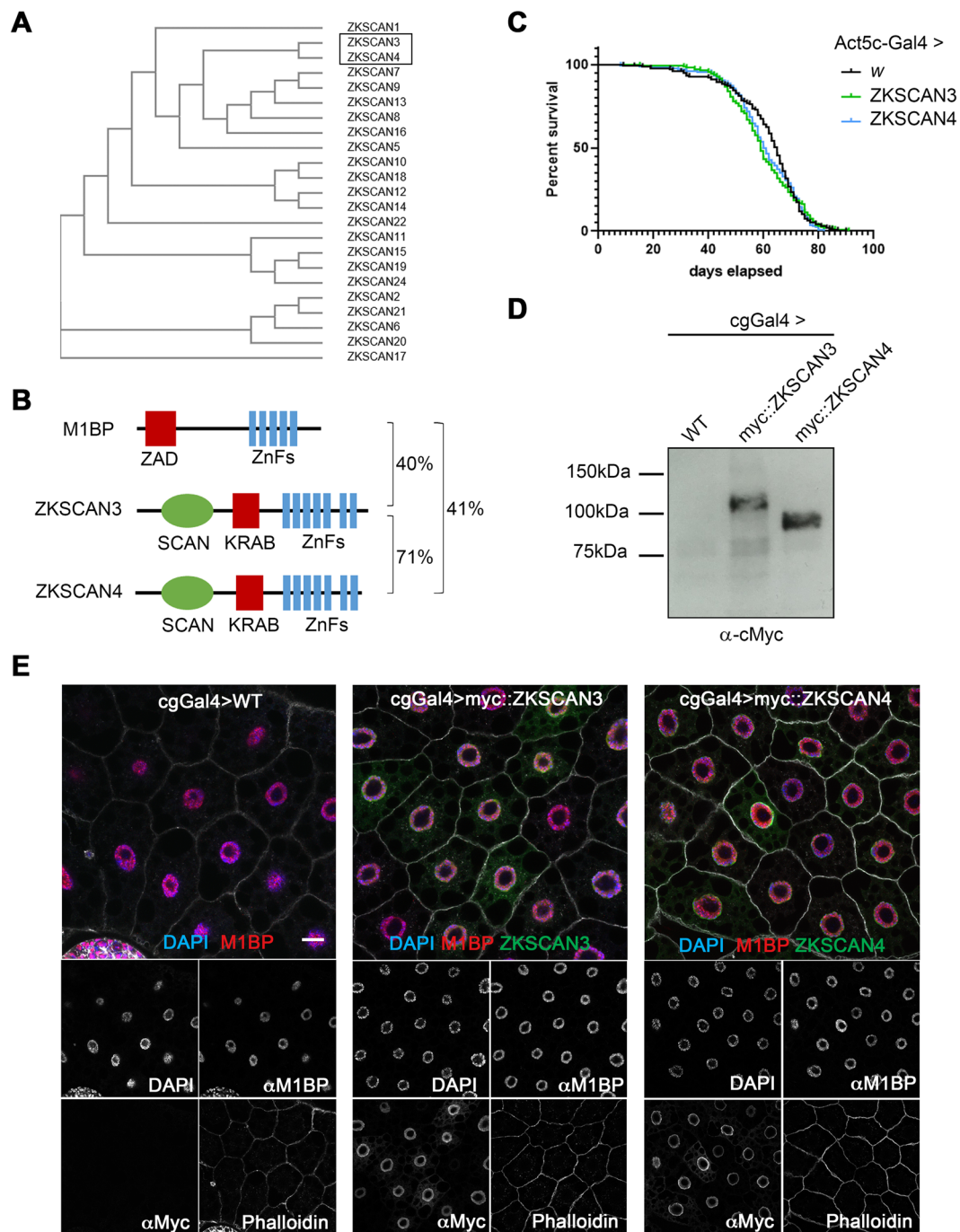
Figure 1. Using Drosophila to study ZKSCAN3 and ZKSCAN4 function in M1BP-controlled processes. (**A**) Phylogenetic tree analysis of primary sequence structure similarity of the vertebrate family of C2H2 zinc finger family transcription factor members containing a SCAN and KRAB domain demonstrates that ZKSCAN3 and ZKSCAN4 are paralogous family members. (**B**) The structural domains of Drosophila M1BP and vertebrate ZSKCAN3 and ZKSCAN4 are shown. C2H2 zinc finger domain clusters are depicted in blue, the SCAN domain, which is not conserved in Drosophila is depicted in green and the evolutionarily analogous ZAD and KRAB domains depicted in red. Percent sequence identity by BLAST conservation searches are shown. (**C**) Drosophila male lifespan was analysed when either ZKSCAN3 or ZKSCAN4 were ubiquitously expressed from the Act5CGal4 driver. No significant change to longevity was observed. (**D**) ZKSCAN3 and ZKSCAN4 expressed in the Drosophila fat body with the cgGal4 driver results in production of full-length protein as determined by western blot analysis. (**E**) Expression of ZKSCAN3 and ZKSCAN4 in the Drosophila fat body with the cgGal4 driver results in nuclear localised exogenous protein localisation (green channels) without changing nuclear M1BP staining (red channel). Nuclei were counterstained with DAPI (blue channel) and cell membranes revealed with Phalloidin (white). Scale bar represents 20 μm and contrasts of individual channels are shown.
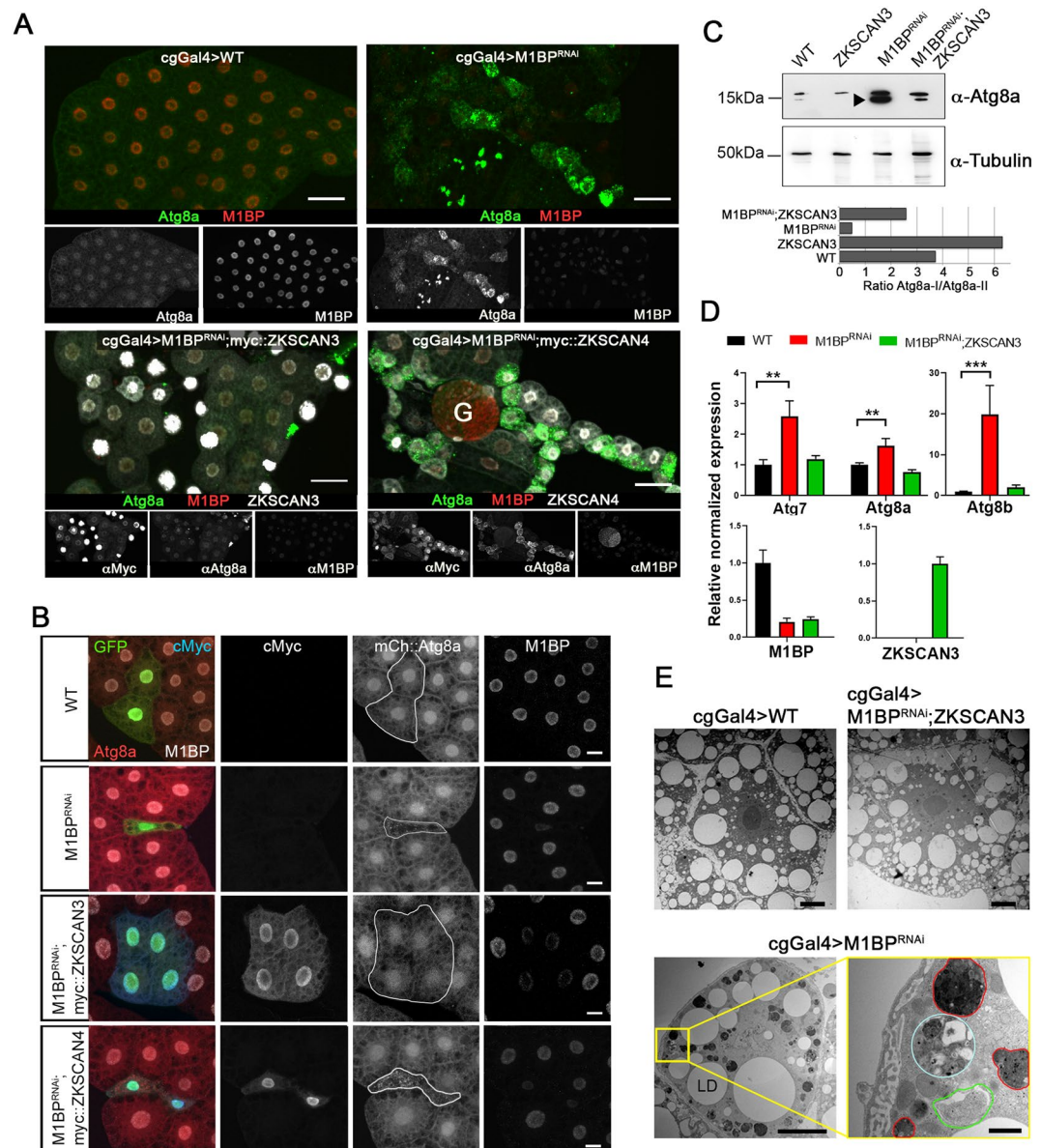
Figure 2. Expression of ZKSCAN3 in the Drosophila fat body prevents induction of autophagy due to loss of M1BP function. (**A**) Upon loss of M1BP expression (red) through expression of M1BP RNAi in L3F fat body cells using the fat body-specific cgGal4 driver, autophagy induction is widespread, as seen by the upregulation and cytoplasmic location of the Atg8a autophagy marker (green). Autophagy induction is largely prevented by the co-expression of myc-tagged vertebrate ZKSCAN3 (bottom left) but not by ZKSCAN4 (bottom right). Contrasts of individual channels are shown and scale bar represents 50 μm. G: Gonad (**B**) Clonal loss, RNAi-expressing cells are GFP-identified and autophagy monitored using mCherry::*Atg8a* confirming that co-expression of myc-tagged ZKSCAN3 can prevent autophagy induction through M1BP knockdown, whereas ZKSCAN4 expression does not. Contrasts of individual channels are shown and scale bars represent 20 μm. (**C**) Western blots of wild type, M1BP RNAi, ZKSCAN3, and M1BP RNAi;ZKSCAN3 expressing whole fat body protein preparations confirm autophagy induction due to M1BP RNAi, through the upregulation of Atg8a expression and the presence of major phosphatidylethanolamine-modified forms of Atg8a (arrowhead), which are largely prevented through ZKSCAN3 co-expression. The blots were reprobed with anti-tubulin antibodies for loading control. Quantification of the ratio of unmodified Atg8a (Atg8a-I) to phosphatidylethanolamine-modified Atg8a (Atg8a-II) is presented below the blots. Note, quantification is of this single unrepeated blot and thus does not incorporate error bars. (**D**) RT-qPCR analyses confirm significant upregulation of autophagy-related Atg gene expression upon M1BP knockdown through M1BP RNAi in the fat body using the cgGal4 driver. Co-expression of ZKSCAN3 prevents Atg gene overexpression without modifying M1BP knockdown. (**E**) Transmission electron micrographs of Drosophila fat body cells display widespread autophagy induction upon M1BP RNAi through the presence of numerous autophagosome vesicles (lower panels) which are largely not observed in wild type cells or cells co-expressing ZKSCAN3 with M1BP RNAi (upper panels). Autophagosomes from all stages of maturity from early phagophore onset (green outline), autophagosomes containing large quantities of cellular material (cyan outline) and late-stage autophagosomes/autolysosomes (red outline) can be observed in M1BP RNAi expressing cells. LD: lipid droplets. Scale bars 10 μm in main micrographs and 1 μm in enlarged area (bottom right).

induced in the L3F stage upon M1BP RNAi (Fig. 2D). Finally, by transmission electron microscopy of fat body cells, we observed large numbers of autophagosomes and late-stage autolysosomes due to M1BP RNAi, which were rarely observed in wild type cells or fat bodies co-expressing ZKSCAN3 (Fig. 2E).

Together, these data demonstrate that the expression of vertebrate ZKSCAN3, but not the paralogous ZKSCAN4, in the Drosophila fat body is sufficient to prevent autophagy induction due to loss of M1BP expression, which we sought to study further.

Loss of M1BP function leads to widespread gene deregulation that is largely restored upon ZKSCAN3 expression. To better understand the transcriptional changes occurring during loss of M1BP function, we performed RNA-seq analyses on fat body mRNA at the L3F stage in the absence and presence of M1BP RNAi. Differential gene expression analyses at a 1:1000 false discovery rate demonstrates that M1BP loss of function leads to the overexpression of 644 genes while down regulating 881 genes (Table S1). Gene set enrichment analyses of M1BP RNAi highlighted biological processes associated with responses to cellular nutrient levels, which include autophagy related genes, in genes that are overexpressed upon M1BP RNAi (Fig. S2A, left panel) and metabolic biological processes were enriched gene ontology terms associated with genes downregulated upon M1BP RNAi (Fig. S2A, right panel). Developmental autophagy induction during the L3 wandering stage (L3W) compared to L3F leads to the deregulation of 3738 genes (1819 upregulated; 1919 downregulated) (Table S1). Comparison of genes deregulated during developmental autophagy induction at the L3W stage with genes deregulated by M1BP RNAi at the L3F stage shows 916 commonly deregulated genes (Fig. S2B). These data demonstrate that M1BP RNAi in the L3F stage deregulates genes that are also deregulated during normal third instar larval development at the L3W stage when autophagy occurs.

Expression of ZKSCAN3 alone in the wild type fat body has little effect on gene expression, with very few genes classed as differentially expressed (Table S1). However, of the 1525 genes differentially expressed due to M1BP RNAi, more than two-thirds (1026) are restored to normal wild type L3F expression levels upon simultaneous co-expression of ZKSCAN3 (Table S1 and Fig. 3A). Amongst these include a number of autophagy-related Atg genes (Fig. 3B). Of note, while the RT-qPCR experiments confirmed changes in expression of Atg7, Atg8a, and Atg8b (Fig. 2D), the RNA-seq expression data gives a more global overview of global Atg gene changes (Fig. 3B) and shows that while indeed Atg8b expression increases in response to M1BP RNAi (and restored upon ZKSCAN3 co-expression) as shown by RT-qPCR, these changes are not significant in the RNA-seq differential gene expression analyses due to the very low level of Atg8b expression. Nonetheless, these data highlight global Atg gene expression changes in response to loss of M1BP expression, and these changes are restored upon ZKSCAN3 coexpression. Similar to the gene set enrichment analysis of enriched gene ontology terms affected by M1BP RNAi (Fig. S2A), Reactome Pathway analysis[36] highlighted us to an enrichment of the Autophagy Reactome for upregulated genes upon M1BP RNAi (30% of Autophagy Reactome entities; Fig. 3C). Focussing on entities specifically within the Macroautophagy Reactome (Reactome Identifier R-DME-1632852), we found that 13 of the 93 Reactome identies (14%) were significantly upregulated upon M1BP RNAi (Table S2). For M1BP RNAi-downregulated genes, we observed significant enrichment of the Metabolism Reactome (23% of Metabolism Reactome entities) (Fig. 3C). The co-expression of ZKSCAN3 with M1BP RNAi restores expression of the majority of these Reactome pathway genes to wild type levels (Fig. 3C). Together, these data demonstrate that M1BP controls thousands of genes in the Drosophila fat body, the majority of which are normally deregulated during larval development and autophagy. Moreover, vertebrate ZKSCAN3 can transcriptionally control the majority of these genes, suggesting that ZKSCAN3 can bind the same genomic targets as M1BP.

ZKSCAN3 binds identical genomic sites as M1BP genome-wide. We sought to compare the genomic binding profiles of ZKSCAN3 and M1BP by genome-wide ChIP-seq analyses. However, using a range of regular chromatin preparation and sonication protocols and kits, we were unable to obtain adequate DNA fragment sizes following fixation and sonication for high-resolution ChIP-seq analyses (data not shown). We believe this is due to the heavy polytinised nature of chromosomes from the Drosophila fat body (256 + copies)[37], which may explain the lack of public whole-genome ChIP datasets from this tissue. Nevertheless, the binding profile of M1BP in Drosophila S2 cell culture cells has been extensively studied[22,38]. Thus to study whether ZKSCAN3 is capable of binding to similar genomic loci as M1BP, we established stable cell lines conditionally expressing HA-tagged ZKSCAN3 and as comparison, HA-tagged ZKSCAN4 (Fig. S3) and performed anti-HA ChIP-seq analyses. Remapping of previous M1BP S2 ChIP-seq datasets[22] to the BDGP Release 6 genome assembly (dm6) and peak calling with highly significant parameters (1% irreproducible discovery rate) identifies 6116 high confidence M1BP-bound genomic regions. Using identical stringent parameters, we identified 8991 ZKSCAN3 bound regions and 8747 ZKSCAN4 bound regions in S2 cells. Eliminating so-called high occupancy target (HOT) regions that appear indiscriminately bound by numerous transcription factors[39], we identified 5279 M1BP peaks, 7884 ZKSCAN3 peaks, and 7734 ZKSCAN4 peaks. Comparing the genomic binding profiles of M1BP with ZKSCAN3 and ZKSCAN4, we observed that of the 5279 HOT-excluded genomic regions bound by M1BP, 87% (4590) are identically targeted by ZKSCAN3 and 52% (2768) are targeted by ZKSCAN4 (Fig. 4A). Surprisingly, of the 2768 M1BP target loci that are also targeted by ZKSCAN4, almost all (94%; 2595 peaks) are also targeted by ZKSCAN3 (Fig. 4B). These data demonstrate that while ZKSCAN4 shares some common M1BP genomic loci, the vast majority of M1BP loci are also loci targeted by ZKSCAN3. Interestingly, of the numerous Atg autophagy genes deregulated in the Drosophila fat body upon M1BP RNAi and rescued by ZKSCAN3 co-expression (Fig. 3B), many of their promoters are also M1BP targets and these promoters are also targeted by ZKSCAN3 (Fig. 4C–E).

Since the DNA recognition sites of ZKSCAN3 and ZKSCAN4 *in vivo* have not been experimentally determined, we performed *de novo* motif discovery on ZKSCAN3 and ZKSCAN4 peaks and found that the most significant overrepresented motif at ZKSCAN3 genomic targets highly resembles the M1BP "Motif 1" binding
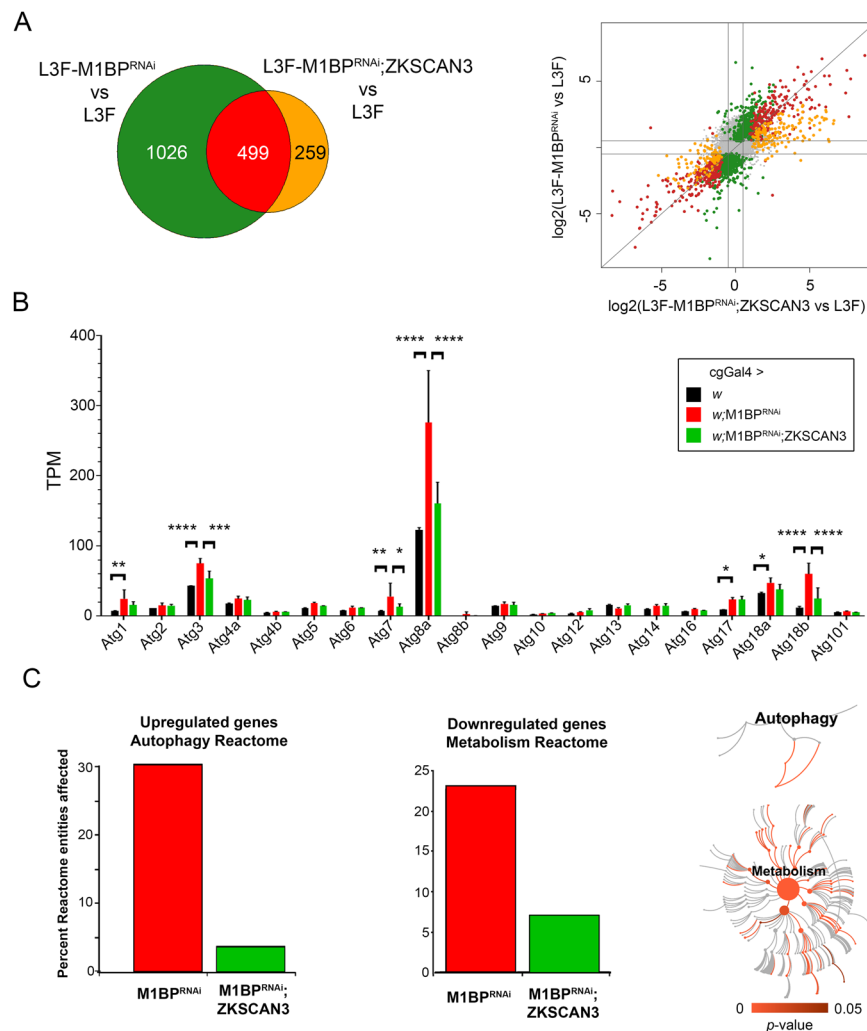
Figure 3. M1BP RNAi leads to widespread gene deregulation that is largely prevented through ZKSCAN3 co-expression. (**A**) Weighted Venn diagram representation of RNA-seq-identified L3F differentially expressed genes (DEGs) upon M1BP RNAi knockdown and DEGs in M1BP RNAi;ZKSCAN3 co-expressing fat body cells highlighting that more than two-thirds (1026) of M1BP RNAi-induced DEGs are prevented by ZKSCAN3 co-expression. Scatter plot of log2 fold changes in gene expression upon M1BP RNAi (ordinate) and M1BP RNAi;ZKSCAN3 (abscissa) co-expressing L3F fat body cells. Differential gene expression analyses identifying DEGs in both conditions are marked in red, genes prevented from being differentially expressed upon M1BP RNAi through ZKSCAN3 co-expression are shown in green and DEGs present in only M1BP RNAi;ZKSCAN3 fat bodies are shown in orange. Genes not differentially expressed in any condition are in grey. (**B**) Average transcripts per million (TPM) from biological replicate RNA-seq counts for all autophagy-related genes (Atg) show significant upregulation of numerous Atg genes upon M1BP RNAi that is prevented by ZKSCAN3 co-expression. Error bars represent standard deviation of mean replicate values. (**C**) Reactome pathway enrichment analysis[36] identified the "Autophagy Reactome" pathway as significantly enriched with 30% of pathway entities being upregulated upon M1BP RNAi and the "Metabolism Reactome" as significantly enriched with 23% of pathway entities being downregulated upon M1BP RNAi. In both cases, the majority of deregulated pathway genes are restored to wild type values upon ZKSCAN3 co-expression leading to the absence of pathway enrichment. The pathway illustrations (CC BY 4.0 license) as provided by the Reactome analyses[36] significantly affected within each of the reactomes are shown in red while not significant pathways are shown in grey.

motif[38], whereas ZKSCAN4 peaks are overrepresented with DNA binding motifs resembling that of GATA transcription factors (Fig. 5A). While ZKSCAN3 and ZKSCAN4 are similar in protein sequence identity (see Fig. 1B), the DNA sequence motif overrepresentation in genomic binding sites is clearly distinct.

While the M1BP binding motif was overrepresented in ZKSCAN3 ChIP-seq peaks, this overrepresentation analysis does not address whether the M1BP Motif 1 binding motif is the DNA recognition site of ZKSCAN3. Studying either the ChIP enrichment at M1BP peaks of all occurrences of Motif 1 (Fig. 5B) or where Motif 1 is localised respective to each ChIP peak summits, representing where the highest quantity of transcription factor binding (Fig. 5C), we found that like M1BP, ZKSCAN3, but not ZKSCAN4, is highly enriched at genomic regions containing and centred on the Motif 1 DNA binding motif. These data suggest that ZKSCAN3 recognises the
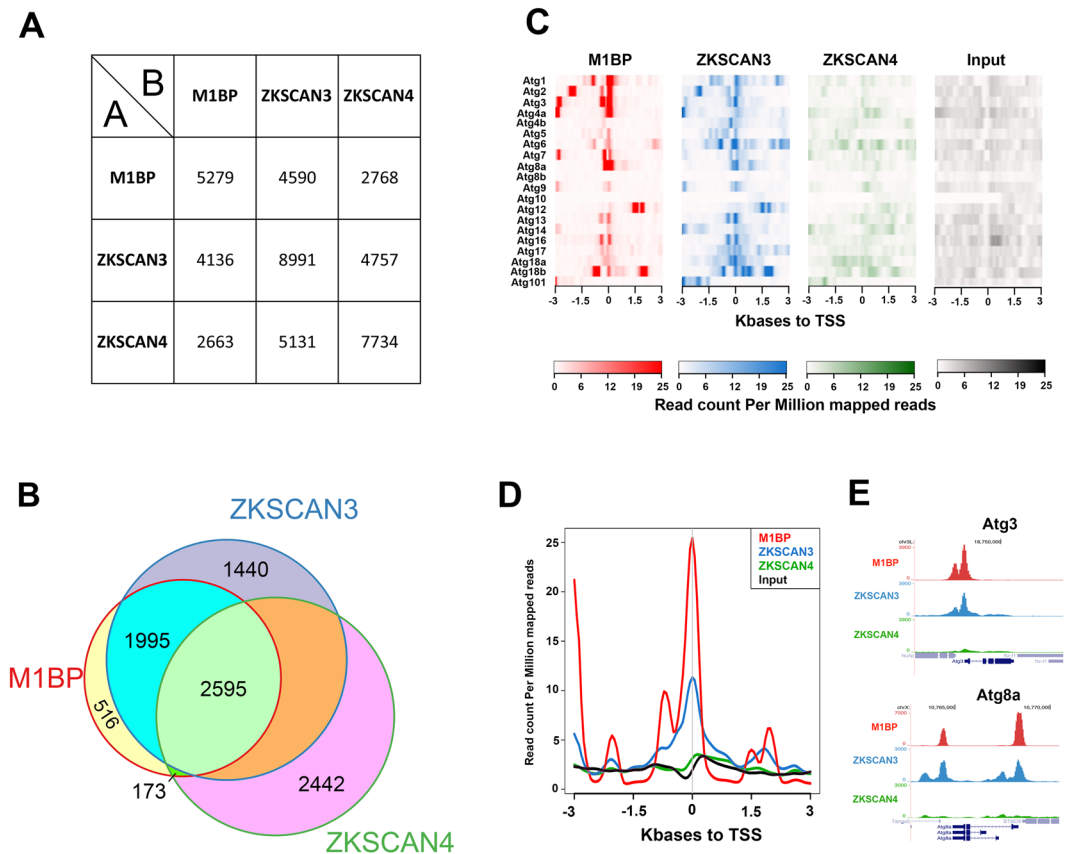
Figure 4. ZKSCAN3 binds identical M1BP genomic targets in Drosophila S2 cells. (**A**) Pairwise ChIP peak intersection analyses is shown with of the number of peaks in the "A" peak datasets (vertical dataset identity) overlapping with peaks of the "B" peak dataset (horizontal dataset identity) displayed. (**B**) Weighted Venn diagram representation of the number of M1BP peaks overlapping with ZKSCAN3, ZKSCAN4 or both ZKSCAN3 and ZKSCAN4 peaks are shown. Since the numbers of peaks change slightly depending on which dataset is used as the source identity (see "A" versus "B" and vice versa in (B) above), only the numbers of peaks not overlapping with any other dataset can be shown for ZKSCAN3 and ZKSCAN4. (**C**) Normalised ChIP sequencing count reads of M1BP, ZKSCAN3, and ZKSCAN4 ChIP and input genomic DNA within a 3-Kb window around the TSS of the 20 Drosophila Atg genes show that M1BP and ZKSCAN3 arestrongly enriched at the promoters of most Atg genes. (**D**) Genomic profiling of normalised ChIP reads of data from (C) showing enrichment of M1BP and ZKSCAN3 at the promoters of Atg genes. (**E**) Genome browser profiles demonstrating that M1BP and ZKSCAN3 target similar autophagy related gene (Atg) promoters in S2 cells.

same DNA element as M1BP. However, it is possible that ZKSCAN3 is not binding Motif 1 directly, but localising to these sites through direct interaction with M1BP. While it isn't possible to perform ZKSCAN3 ChIP in the absence of M1BP, due to either premature autophagy induction[22] or cell cycle arrest[40] upon M1BP knockdown, we believe that ZKSCAN3 binding to Motif 1 is not simply through protein-protein interaction with M1BP, since we observed no ZKSCAN3-specific direct interaction with M1BP (Fig. 5D).

These data suggest that M1BP and ZKSCAN3 are likely direct repressors of autophagy-related gene expression, whereby loss of M1BP/ZKSCAN3 function leads to Atg upregulation, which is essential for both autophagy induction and progression[41]. Thus, given that ZKSCAN3 can target identical genomic regions as M1BP in Drosophila cell lines and can restore the expression of the majority of genes deregulated through M1BP RNAi in Drosophila fat body tissue, these data strongly suggest that ZKSCAN3 replaces M1BP function in autophagy repression through similar transcriptional mechanisms employed by M1BP and not simply as an alternative repressor of autophagy.

M1BP can repress autophagy induction due to cytoplasmic ZKSCAN3 translocation in vertebrates.
In vertebrates, autophagy is induced under lysosomal stress and starvation conditions due to the relocalisation of ZKSCAN3 from the nucleus to cytoplasm[16]. To further investigate the interchangeable nature of M1BP and ZKSCAN3 function in the control of autophagy, we asked whether Drosophila M1BP could functionally replace ZKSCAN3 in autophagy repression under starvation conditions in vertebrates. Using LC3A as an autophagy marker, under starvation conditions, autophagy is induced in vertebrate cells through the relocation of ZKSCAN3 from the nucleus to the cytoplasm (Fig. 6A,B and Chauhan, *et al.*[16]). We found that transfected Drosophila M1BP is nuclear, even under starvation conditions (Fig. 6C). This nuclear localisation of M1BP
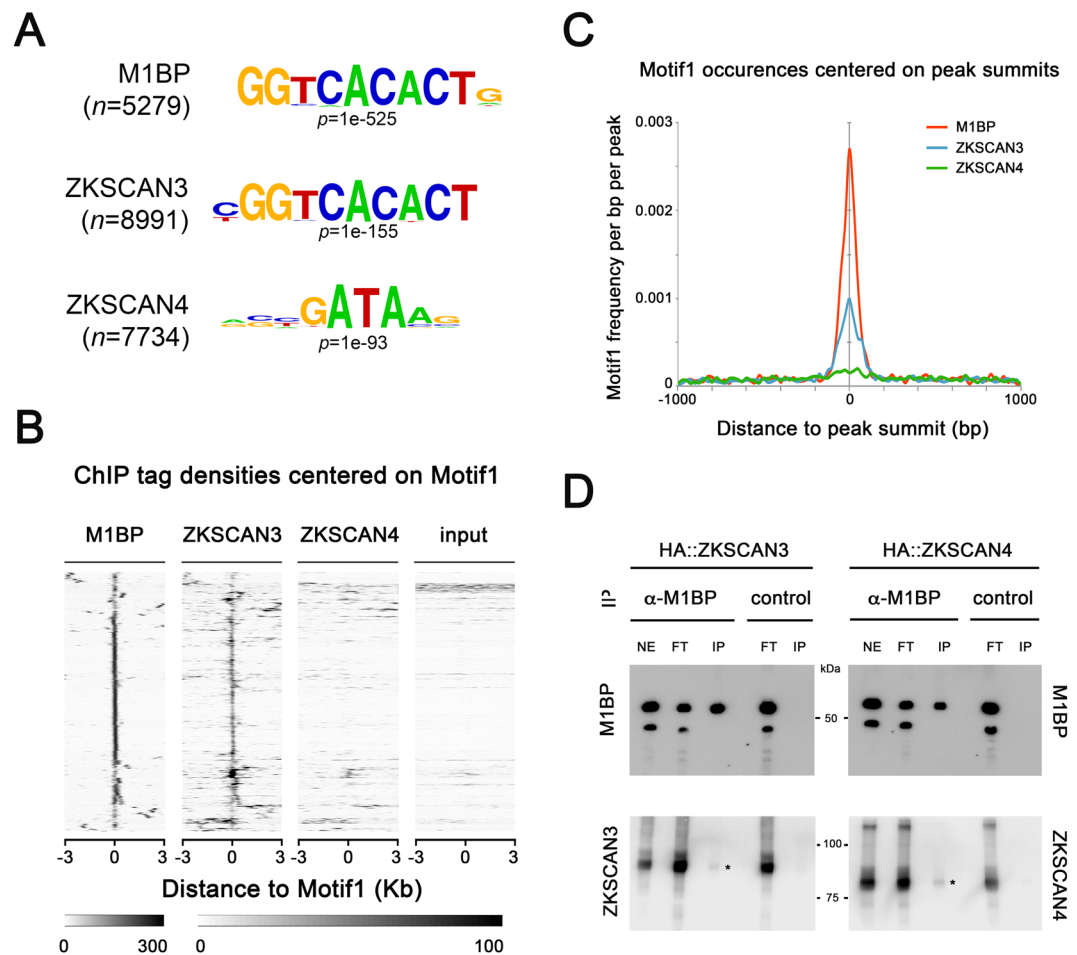
Figure 5. ZKSCAN3 binds the same Motif 1 DNA motif as M1BP. (**A**) The most significant DNA sequence motif found by *de novo* motif discovery analyses on high confidence called peaks (1% irreproducible discovery rate) of M1BP ($n = 5279$ peaks), ZKSCAN3 ($n = 7884$ peaks), and ZKSCAN4 ($n = 7734$ peaks) ChIP-seq profiles shows that Motif 1 DNA element[57] is significantly enriched at ZKSCAN3 and M1BP peaks. (**B**) Sequence tag densities of M1BP, ZKSCAN3 and ZKSCAN4 ChIP and input DNA centred on Motif1 at M1BP peaks shows that ZKSCAN3, but not ZKSCAN4 preferentially targets Motif 1 DNA sequences in Drosophila. (**C**) The frequency of Motif 1 position weight matrix occurrences on all M1BP, ZKSCAN3, and ZKSCAN4 ChIP peak summits show that like M1BP, Motif 1 is enriched at ZKSCAN3 ChIP peak summit binding locations. (**D**) ZKSCAN3 and ZKSCAN4 show little physical interaction with M1BP. M1BP was immunoprecipitated from HA::ZKSCAN3 and HA::ZKSCAN4-expressing Drosophila cell lines and probed for ZKSCAN3 or ZKSCAN4 interaction with anti-HA antisera. The low levels of both ZKSCAN3 and ZKSCAN4 interacting with M1BP (asterisks) cannot explain the ZKSCAN3-specific binding to Motif 1, since both both ZKSCAN3 and ZKSCAN4 were immunoprecipitated at equal amounts.

was sufficient to significantly inhibit autophagy induction, where cytoplasmic LC3A accumulation is inhibited (Fig. 6D) and autophagy related gene expression is restored (Fig. 6E). M1BP binds a highly stringent DNA sequence of nine nucleotides, called Motif1 (Ref. [38] and see Fig. 5A). To better understand how Drosophila M1BP can transcriptionally regulate these vertebrate autophagy genes, we performed bioinformatics analyses of the promoters of known vertebrate Atg transcripts ($n = 48$). We found that nearly all (46/48) of these Atg transcripts contained a highly significant match for Motif1 within their promoters (Table S3), suggesting that Drosophila M1BP can bind this promoter sequence in vertebrates to regulate autophagy gene expression. These data suggest starvation-induced autophagy due to the cytoplasmic relocation of ZKSCAN3 can be prevented through the function of Drosophila M1BP in the nucleus.

Collectively, these data demonstrate that vertebrate ZKSCAN3 and Drosophila M1BP are homologous transcription factors that bind similar genomic sequences in Drosophila and can functionally replace each other in autophagy repression.

Discussion

Autophagy is a tightly controlled cellular process that is essential in maintaining cellular homeostasis and can play a protective or destructive role in disease. Thus, identifying the factors and mechanisms at the heart of autophagy repression is essential for anti-cancer therapeutic targeting[42]. The identification of ZKSCAN3 as a master repressor of autophagy induction[16] provides a potential therapeutic anti-cancer target, particularly in cancers that
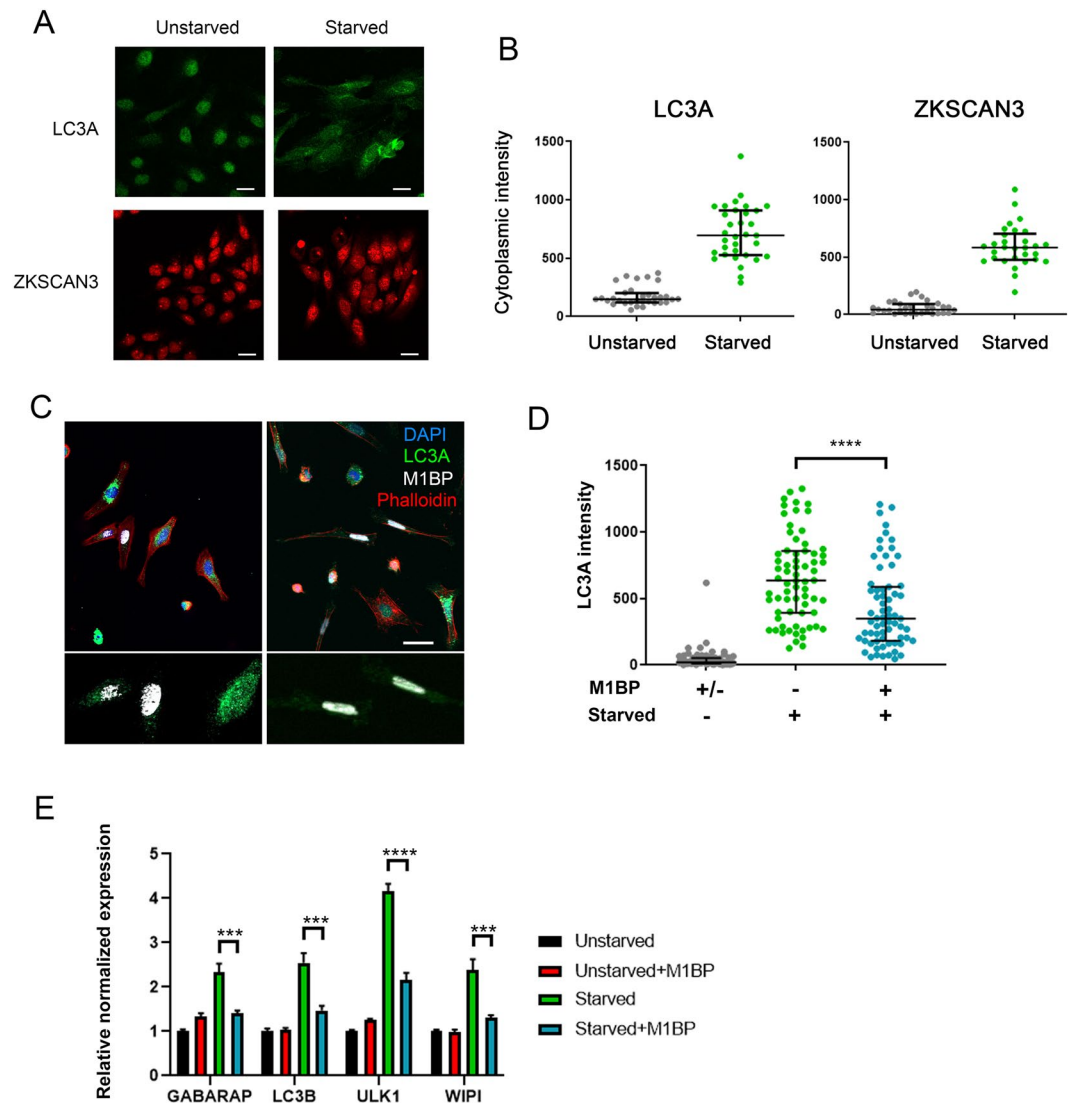
Figure 6. M1BP expression can prevent starvation-induced autophagy when expressed in vertebrate cells. (**A**) Representative immunofluorescent staining of unstarved and starved HeLa cells showing increased cytoplasmic staining of LC3A (green) and ZKSCAN3 upon starvation. Scale 25 μm. (**B**) Quantification of cytoplasmic immunofluorescence signal of LC3A and ZKSCAN3 in unstarved and starved HeLa cells confirming autophagy induction through the shuttling of ZKSCAN3 into the cytoplasm. (**C**) Representative immunofluorescence staining of LC3A (green) in independent experiments of starved HeLa cells demonstrates that cells containing transiently transfected M1BP (white) display generally lower levels of cytoplasmic LC3A accumulation. Nuclei are counterstained with DAPI (blue) and cell membranes marked with Phalloidin (red). Enlarged views of M1BP-transfected cells showing diminished cytoplasmic LC3A staining are shown below the main images. Scale 50 μm. (**D**) Quantification of cytoplasmic LC3A immunofluorescence signal in unstarved and starved HeLa cells demonstrates significant reduction of cytoplasmic LC3A in cells transiently transfected with M1BP. (**E**) RT-qPCR analyses of key vertebrate autophagy genes induced upon HeLa cell starvation demonstrate induction of expression is significantly inhibited in cells transiently transfected with M1BP.

inactivate nuclear ZKSCAN3 function for autophagy induction and increased energy production[43]. A *Zkscan3* knock-out mouse model, displaying no apparent autophagy-related phenotypes questioned whether ZKSCAN3 was a repressor of autophagy induction in animal tissue, outside of the transformed cell line *in vitro* model within which is autophagy repressive function was demonstrated[18]. Here, we show that vertebrate ZKSCAN3 is capable of repressing premature autophagy induction in developing Drosophila tissue. Importantly, we show that ZKSCAN3 transcriptionally restores normal autophagy-related gene expression induced by loss of M1BP function (Fig. 3B), most likely through direct binding to their promoters (Fig. 4C), providing important potential mechanistic insight into how ZKSCAN3 can inhibit autophagy induction. Furthermore, identifying the preferred binding sequence motifs of ZKSCAN3 affords an explanation as to how ZKSCAN3 can functionally replace M1BP in autophagy repression, through binding identical genomic sequences.

These data demonstrate that ZKSCAN3 can regulate autophagic processes in a developing animal and that this function is evolutionary conserved. It has also been suggested that the absence of autophagy phenotypes in the *Zkscan3* knock-out mouse model may be due to functional compensation by the paralogous Zkscan4 protein[18]. Our data demonstrate that ZKSCAN4 in Drosophila, is not capable of repressing autophagy from loss of M1BP function. However, given that insect-specific ZAD-domain in M1BP has much evolved to give rise to the vertebrate KRAB domain in ZKSCAN3/4[23–25], it is possible that the highly related *ZKSCAN3* and *ZKSCAN4* genes are both evolutionary homologues of Drosophila M1BP, but only ZKSCAN3 has retained the ability to repress autophagy in the manor performed by Drosophila M1BP. This would allow the hypothesis that in the natural vertebrate context, ZKSCAN4 can compensate for loss of ZKSCAN3 function in autophagy repression, yet when challenged in an evolutionary ancient model system, only ZKSCAN3 is capable of performing this task.

In the regulation of autophagy, it is noteworthy that in order to induce autophagy, the cellular mechanisms employed by Drosophila and vertebrates would appear to have evolved: In Drosophila, the nuclear function of both M1BP and Hox transcription factors are mutually required to prevent autophagy induction[22] whereby Drosophila clear all Hox function to induce autophagy during development or under starvation conditions[15]; in vertebrates, while the underlying reasons remain unknown, the mechanisms of autophagy induction have evolved to require the nuclear eviction of ZKSCAN3 by JNK2/p38-mediated phosphorylation of Thr153 within a nuclear export signal sequence[16,17], a sequence which is not conserved in Drosophila M1BP (data not shown).

M1BP is known to bind promoters of genes with gene ontology terms linked to metabolism[22,38] and our data show that metabolic gene expression is lost upon M1BP knockdown (Figs. S2A and 3C) suggesting that M1BP promoter binding to these genes actively controls their expression. Thus, since loss of M1BP expression leads to loss of metabolic gene expression and that changes in cellular metabolism are well known to induce autophagy[44,45], this could be the cellular signal that leads to autophagy induction upon loss of M1BP function. Given that ZKSCAN3 transcriptionally rescues defects in metabolic gene transcription due to M1BP RNAi (Fig. 3C), this also suggests that, like M1BP, ZKSCAN3 regulates metabolic gene expression. From a mechanistic point of view, the sharing of promoter binding sequences and gene regulation by M1BP and ZKSCAN3 also suggests that both proteins control gene expression though similar molecular mechanism. As M1BP controls transcription through RNA Pol II pausing[38], ZKSCAN3 may also control this process, a hypothesis that remains to be tested.

Finally, as ZKSCAN3 dysregulation contributes to numerous human cancers[43,46–51] and that metabolic reprogramming is a hallmark of the tumour microenvironment (reviewed in[52]), the knowledge that Drosophila M1BP and vertebrate ZKSCAN3 are functionally homologous proteins controlling autophagy and metabolic gene expression will allow use of the powerful Drosophila model system to study ZKSCAN3 function in metabolism, autophagy control and cancerogenesis.

Materials and Methods

Fly stocks. The following lines UAS-3xmyc::ZKSCAN3 and UAS-3xmyc::ZKSCAN4 were established by using a pUAST plasmid encoding 3xmyc epitope tag (p131) and cDNA of vertebrate ZKSCAN3 variant 1 (NM_001145778.1) and ZKSCAN4 (IMAGE clone 4336904). Drosophila injections for establishing the ZKSCAN3 and ZKSCAN4 UAS fly lines were performed by TheBestGene (USA). For M1BP loss of function the line UAS-M1BP^RNAi 30016kk was obtained from the Vienna Drosophila Stock center. The fat body specific cgGal4 (Bloomington 7011) and ubiquitous Act5C-Gal4 (Bloomington 3954) driver lines was obtained from the Bloomington stock centre. For clonal analysis, the *y w hsflp; r4-mCherry-Atg8a Act > CD2 > GAL4 UAS-GFPnls* fly stock was used (a gift from T.Neufeld).

Imaging. For immunofluorescences, around 10 larval fat bodies are dissected per condition in 0.01 M PBS/0,7% NaCl, fixed for 1 h in 1.8% formaldehyde in PBS and washed for 10 min in PBS followed by 15 min in PBTX-DOC (PBS, 0.1% Triton X-100, 0.05% DOC). After 1 H of blocking in 1% BSA/PBTX-DOC, fat bodies were incubated overnight with primary antibodies at 4 °C. Following 3 × 30 min washes with PBTX-DOC, secondary antibodies were added for 1 H. After washing for 1 H in PBTX-DOC followed by 15 min in PBS, fat bodies were mounted in Vectashield and visualised using confocal (Zeiss LSM 880) or apotome (Zeiss AxioImager APO M2) fluorescence microscopy.

Transmission electron microscopy of fat bodies from larvae of cgGal4 > UAS-M1BP^RNAi, cgGal4 > UAS-M1BP^RNAi; ZKSCAN3 and control cgGal4 > + were dissected, fixed and processed as described in[15].

Antibodies. The following primary antibodies were used: rat anti-atg8a (a gift from G. Jusász), rabbit anti-M1BP[22], mouse anti-c-Myc (9E10; Santa Cruz Biotech; SC-40), mouse anti-His (Abcam; ab9136) and rabbit anti-LC3A (Cell Signaling Techology).

Quantitative RT-PCR. Total RNA was isolated from 10 fat bodies of males (gonads removed) in L3F with the RNeasy Mini Kit (Qiagen) and either sent for RNA-seq, after verification of the RNA quality on Bioanalyser (Agilent), or the RNA was reversed transcribed to cDNA by using the SuperScript III according to the manufacturer's instructions (Life Technologies). qRT-PCR was carried out with SYBR green mix (Life Technologies) and performed in triplicate on CFX96 thermocycler (BioRad). Data and statistical tests were analysed on CFX manager software (BioRad).

The following Drosophila-specific primers were used for qRT-PCR on fat bodies:
M1BP F: CGCATGGCCTTTGAACTT
M1BP R: GAAGCGCGACTGACAGAGTT
Atg8a F: GGGAGCCTTCTCGACGAT
Atg8a R: TTCATTGCAATCATGAAGTTCC
Atg8b F: CGGTGGGATCACATTGTTTA

Atg8b R: ATCCGCAAGCGTATCAATCT
Atg7 F: GGCTGTCATCGATGTTCATTT
Atg7 R: TTTCTGCTTCAGCAATGTCC
ZKSCAN3 F: AGCAGGATTCATCTCAGGGGA
ZKSCAN3 R: ACTCTTTCCACATTCATGGCAGA
ZKSCAN4 F: GGTGGTGGTGCTATTGGAGT
ZKSCAN4 R: GTCACCAACGGGAACCTG
U6 F: CGATACAGAGAAGATTAGCATGGC
U6 R: GATTTTGCGTGTCATCCTTGC
Rp49 F: CGCTTCAAGGGACAGTATCTG
RP49 R: AAACGCGGTTCTGCATGA
Actin5c F: TCAGTCGGTTTATTCCAGTCATTCC
Actin5c R: CCAGAGCAGCAACTTCTTCGTCA

ChIP-seq experiments. S2-DRSC cells (Drosophila Genomics Resource Center, stock #181) were cultured at 25 °C in Schneider's medium (Clinisciences) supplemented with 10% FBS. HA-tagged ZKSCAN3 or ZKSCAN4 were cloned into pMK33/pMtHy (Drosophila Genomics Resource Center), transfected into S2-DRSC cells and stable lines generated through Hygromycin B selection over a 4-week period. ZKSCAN3 or ZKSCAN4 were induced with 100 μm $CuSO_4$ addition to the media for 48 h before chromatin preparations and anti-HA ChIP performed as previously described[22]. Anti-HA ChIP-seq on untransfected and $CuSO_4$-induced S2 cells has previously been performed yielding no significant anti-HA ChIP peaks[22].

High-throughput sequencing and analysis. Sequencing was performed on libraries prepared from duplicates of ChIP or RNA preparations. RNA-seq libraries were prepared using the TruSeq RNA Sample Preparation Kit (Illumina) and ChIP-seq libraries were prepared using theMicroPlex Library Preparation Kit (Diagenode) following the manufacturer's instructions. All libraries were validated for concentration and fragment size using Agilent DNA1000 chips. Sequencing was performed on a HiSeq. 4000 or Next-seq. 500 sequencer (Illumina) using a 150-nt paired-end protocol. Base calling performed using RTA (Illumina) and quality control performed using FastQC.

M1BP S2 ChIP-seq sequences were previously generated (GSE101557) and remapped to the dm6 UCSC Drosophila genome release using Subread Aligner[53] (version 1.6.1) resulting in an average of 14.1×10^6 mapped reads from both replicates. ZKSCAN3 and ZKSCAN4 ChIP-seq sequences were mapped to the dm6 UCSC Drosophila genome release resulting in an average of 42.8×10^6 ZKSCAN3 and 35.6×10^6 ZKSCAN4 mapped reads per replicate. High confidence binding sites were determined through peak calling using MACS2 (version 2.1.1.20160309) using an irreproducible discovery rate (IDR) of 1% for all ChIP-seq data as outlined by the ENCODE and modENCODE consortium using each biological replicate. IDR peaks localising to HOT regions were removed resulting in 5279 M1BP peaks, 7884 ZKSCAN3 peaks and 7734 ZKSCAN4 peaks. Comparison of binding of ZKSCAN3 and ZKSCAN4 to M1BP genomic targets was performed using BEDTools[54] "intersect" using M1BP peaks as the "A" dataset and ZKSCAN3 or ZKSCAN4 peaks as the "B" dataset to allow direct comparison of co-targeted regions.

De novo motif discovery was performed on all high confidence M1BP, ZKSCAN3, and ZKSCAN4 peak region centers in S2 cells using Homer. Similarity matching of identified motifs with known motifs was performed using STAMP and the most significant overrepresented motif shown.

Analysis of Motif1 binding site matches in the promoters of vertebrate Atg genes was performed using FIMO of the MEME SUIT of tools[55].

For RNA-seq analyses, raw counts from RNA-seq were obtained using featureCounts from the Subread package[53] (Version 1.6.1). Differentially expressed genes were called using DESeq2[56] (version 1.14.1) using a false discovery rate (p-adjusted value in DESeq2) threshold of 0.001.

Vertebrate cell culture. HeLa cell line was cultured at 37 °C with 5% CO_2 in Dubelcco's modified Eagle's medium (DMEM) supplemented with 1% FBS from ATCC. Transient transfection was performed with X-tremeGENE™ HP DNA Transfection Reagent (Sigma-Aldrich) following the manufacturer's instructions. For starvation, cells were cultured for 4 H in DMEM without amino acid and with a low concentration of glucose as previously described[15].

For qRT-PCR, 0.5×10^6 cells were seeded and extracted as described above. The following primers were used:
M1BP F: CGCATGGCCTTTGAACTT
M1BP R: GAAGCGCGACTGACAGAGTT
LC3B F: CGCACCTTCGAACAAAGAG
LC3B R: CTCACCCTTGTATCGTTCTATTATCA
ULK1 F: CAGACGACTTCGTCATGGTC
ULK1 R: AGCTCCCACTGCACATCAG
GABARAP F: CGGGTGCCGGTGATAGTAGA
GABARAP R: TGAGATCAGAAGGCACCAGGTA
WIPI F: TCAAACTCGAGACTGTGAAAGAAA
WIPI R: AGCACTTTCCCGAAGTACCC
ZKSCAN3 F: TTCATCTCAGGGGAATCTCTG
ZKSCAN3 R: GAGGCAAGTCCCTGCTCTTA
GAPDH F: GTCAAGGCTGAGAACGGGAA
GAPDH R: AAATGAGCCCCAGCCTTCTC

B-actin F: AGAGCTACGAGCTGCCTGAC
B-actin R: AGCACTGTGTTGGCGTACAG
RNA18S F: CCGATTGGATGGTTTAGTGAG
RNA18S R: AGTTCGACCGTCTTCTCAGC

Data availability

References

1. Devkota, S. The autophagy process. *Oncotarget* **8**, 18623, https://doi.org/10.18632/oncotarget.15951 (2017).
2. Parzych, K. R. & Klionsky, D. J. An overview of autophagy: morphology, mechanism, and regulation. *Antioxid Redox Signal* **20**, 460–473, https://doi.org/10.1089/ars.2013.5371 (2014).
3. Goldsmith, J., Levine, B. & Debnath, J. Autophagy and cancer metabolism. *Methods Enzymol* **542**, 25–57, https://doi.org/10.1016/B978-0-12-416618-9.00002-9 (2014).
4. Hou, X., Watzlawik, J. O., Fiesel, F. C. & Springer, W. Autophagy in Parkinson's Disease. *J. Mol. Biol.*, https://doi.org/10.1016/j.jmb.2020.01.037 (2020).
5. Kim, J., Lim, Y. M. & Lee, M. S. The Role of Autophagy in Systemic Metabolism and Human-Type Diabetes. *Mol Cells* **41**, 11–17, https://doi.org/10.14348/molcells.2018.2228 (2018).
6. Levine, B. & Kroemer, G. Biological Functions of Autophagy Genes: A Disease Perspective. *Cell* **176**, 11–42, https://doi.org/10.1016/j.cell.2018.09.048 (2019).
7. Wang, Y. & Zhang, H. Regulation of Autophagy by mTOR Signaling Pathway. *Adv Exp Med Biol* **1206**, 67–83, https://doi.org/10.1007/978-981-15-0602-4_3 (2019).
8. Corona Velazquez, A. F. & Jackson, W. T. So Many Roads: the Multifaceted Regulation of Autophagy Induction. *Molecular and cellular biology* **38**, https://doi.org/10.1128/MCB.00303-18 (2018).
9. Fullgrabe, J., Klionsky, D. J. & Joseph, B. The return of the nucleus: transcriptional and epigenetic control of autophagy. *Nature reviews* **15**, 65–74, https://doi.org/10.1038/nrm3716 (2014).
10. Hu, L. F. Epigenetic Regulation of Autophagy. *Adv Exp Med Biol* **1206**, 221–236, https://doi.org/10.1007/978-981-15-0602-4_11 (2019).
11. Fullgrabe, J., Ghislat, G., Cho, D. H. & Rubinsztein, D. C. Transcriptional regulation of mammalian autophagy at a glance. *J Cell Sci* **129**, 3059–3066, https://doi.org/10.1242/jcs.188920 (2016).
12. Pietrocola, F. *et al.* Regulation of autophagy by stress-responsive transcription factors. *Semin Cancer Biol* **23**, 310–322, https://doi.org/10.1016/j.semcancer.2013.05.008 (2013).
13. Settembre, C. *et al.* TFEB controls cellular lipid metabolism through a starvation-induced autoregulatory loop. *Nat Cell Biol* **15**, 647–658, https://doi.org/10.1038/ncb2718 (2013).
14. Bouche, V. *et al.* Drosophila Mitf regulates the V-ATPase and the lysosomal-autophagic pathway. *Autophagy* **12**, 484–498, https://doi.org/10.1080/15548627.2015.1134081 (2016).
15. Banreti, A., Hudry, B., Sass, M., Saurin, A. J. & Graba, Y. Hox proteins mediate developmental and environmental control of autophagy. *Developmental cell* **28**, 56–69, https://doi.org/10.1016/j.devcel.2013.11.024 (2014).
16. Chauhan, S. *et al.* ZKSCAN3 is a master transcriptional repressor of autophagy. *Mol Cell* **50**, 16–28, https://doi.org/10.1016/j.molcel.2013.01.024 (2013).
17. Li, Y., *et al.* Protein kinase C controls lysosome biogenesis independently of mTORC1. *Nat Cell Biol* **18**, 1065–1077, https://doi.org/10.1038/ncb3407 (2016).
18. Pan, H., Yan, Y., Liu, C. & Finkel, T. The role of ZKSCAN3 in the transcriptional regulation of autophagy. *Autophagy* **13**, 1235–1238, https://doi.org/10.1080/15548627.2017.1320635 (2017).
19. Chandra, V., Bhagyaraj, E., Parkesh, R. & Gupta, P. Transcription factors and cognate signalling cascades in the regulation of autophagy. *Biol Rev Camb Philos Soc* **91**, 429–451, https://doi.org/10.1111/brv.12177 (2016).
20. Lapierre, L. R. *et al.* The TFEB orthologue HLH-30 regulates autophagy and modulates longevity in Caenorhabditis elegans. *Nature communications* **4**, 2267, https://doi.org/10.1038/ncomms3267 (2013).
21. Safra, M. *et al.* The FOXO transcription factor DAF-16 bypasses ire-1 requirement to promote endoplasmic reticulum homeostasis. *Cell metabolism* **20**, 870–881, https://doi.org/10.1016/j.cmet.2014.09.006 (2014).
22. Zouaz, A. *et al.* The Hox proteins Ubx and AbdA collaborate with the transcription pausing factor M1BP to regulate gene transcription. *EMBO J* **36**, 2887–2906, https://doi.org/10.15252/embj.201695751 (2017).
23. Chung, H. R., Schafer, U., Jackle, H. & Bohm, S. Genomic expansion and clustering of ZAD-containing C2H2 zinc-finger genes in Drosophila. *EMBO reports* **3**, 1158–1162, https://doi.org/10.1093/embo-reports/kvf243 (2002).
24. Lespinet, O., Wolf, Y. I., Koonin, E. V. & Aravind, L. The role of lineage-specific gene family expansion in the evolution of eukaryotes. *Genome Res* **12**, 1048–1059, https://doi.org/10.1101/gr.174302 (2002).
25. Looman, C., Abrink, M., Mark, C. & Hellman, L. KRAB zinc finger proteins: an analysis of the molecular mechanisms governing their increase in numbers and complexity during evolution. *Mol Biol Evol* **19**, 2118–2130, https://doi.org/10.1093/oxfordjournals.molbev.a004037 (2002).
26. Duffy, J. B. GAL4 system in Drosophila: a fly geneticist's Swiss army knife. *Genesis* **34**, 1–15, https://doi.org/10.1002/gene.10150 (2002).
27. Lorincz, P., Mauvezin, C. & Juhasz, G. Exploring Autophagy in Drosophila. *Cells* **6**, https://doi.org/10.3390/cells6030022 (2017).
28. McPhee, C. K. & Baehrecke, E. H. Autophagy in Drosophila melanogaster. *Biochim Biophys Acta* **1793**, 1452–1460, https://doi.org/10.1016/j.bbamcr.2009.02.009 (2009).
29. Scott, R. C., Schuldiner, O. & Neufeld, T. P. Role and regulation of starvation-induced autophagy in the Drosophila fat body. *Developmental cell* **7**, 167–178, https://doi.org/10.1016/j.devcel.2004.07.009 (2004).
30. Li, J. *et al.* ZNF307, a novel zinc finger gene suppresses p53 and p21 pathway. *Biochemical and Biophysical Research Communications* **363** (4), 895–900 (2007).
31. Shpilka, T., Weidberg, H., Pietrokovski, S. & Elazar, Z. Atg8: an autophagy-related ubiquitin-like protein family. *Genome biology* **12**, 226, https://doi.org/10.1186/gb-2011-12-7-226 (2011).
32. Kim, J., Dalton, V. M., Eggerton, K. P., Scott, S. V. & Klionsky, D. J. Apg7p/Cvt2p is required for the cytoplasm-to-vacuole targeting, macroautophagy, and peroxisome degradation pathways. *Mol Biol Cell* **10**, 1337–1351, https://doi.org/10.1091/mbc.10.5.1337 (1999).

33. Kirisako, T. *et al*. Formation process of autophagosome is traced with Apg8/Aut7p in yeast. *J Cell Biol* **147**, 435–446, https://doi.org/10.1083/jcb.147.2.435 (1999).
34. Tanida, I. *et al*. Apg7p/Cvt2p: A novel protein-activating enzyme essential for autophagy. *Mol Biol Cell* **10**, 1367–1379, https://doi.org/10.1091/mbc.10.5.1367 (1999).
35. Ichimura, Y. *et al*. A ubiquitin-like system mediates protein lipidation. *Nature* **408**, 488–492, https://doi.org/10.1038/35044114 (2000).
36. Fabregat, A. *et al*. Reactome pathway analysis: a high-performance in-memory approach. *BMC Bioinformatics* **18**, 142, https://doi.org/10.1186/s12859-017-1559-2 (2017).
37. Richards, G. The polytene chromosomes in the fat body nuclei of Drosophila melanogaster. *Chromosoma* **79**, 241–250 (1980).
38. Li, J. & Gilmour, D. S. Distinct mechanisms of transcriptional pausing orchestrated by GAGA factor and M1BP, a novel transcription factor. *EMBO J* **32**, 1829–1841, https://doi.org/10.1038/emboj.2013.111 (2013).
39. Boyle, A. P. *et al*. Comparative analysis of regulatory information and circuits across distant species. *Nature* **512**, 453–456, https://doi.org/10.1038/nature13668 (2014).
40. Baumann, D. G., Dai, M. S., Lu, H. & Gilmour, D. S. GFZF, a Glutathione S-Transferase Protein Implicated in Cell Cycle Regulation and Hybrid Inviability, Is a Transcriptional Coactivator. *Molecular and cellular biology* **38**, https://doi.org/10.1128/MCB.00476-17 (2018).
41. Yu, L., Chen, Y. & Tooze, S. A. Autophagy pathway: Cellular and molecular mechanisms. *Autophagy* **14**, 207–215, https://doi.org/10.1080/15548627.2017.1378838 (2018).
42. Dolgin, E. Anticancer autophagy inhibitors attract 'resurgent' interest. *Nat Rev Drug Discov* **18**, 408–410, https://doi.org/10.1038/d41573-019-00072-1 (2019).
43. Li, S. *et al*. Transcriptional regulation of autophagy-lysosomal function in BRAF-driven melanoma progression and chemoresistance. *Nature communications* **10**, 1693, https://doi.org/10.1038/s41467-019-09634-8 (2019).
44. Rabinowitz, J. D. & White, E. Autophagy and metabolism. *Science* **330**, 1344–1348, https://doi.org/10.1126/science.1193497 (2010).
45. Galluzzi, L., Pietrocola, F., Levine, B. & Kroemer, G. Metabolic control of autophagy. *Cell* **159**, 1263–1276, https://doi.org/10.1016/j.cell.2014.11.006 (2014).
46. Chi, Y. *et al*. ZKSCAN3 promotes breast cancer cell proliferation, migration and invasion. *Biochem Biophys Res Commun* **503**, 2583–2589, https://doi.org/10.1016/j.bbrc.2018.07.019 (2018).
47. Kawahara, T. *et al*. ZKSCAN3 promotes bladder cancer cell proliferation, migration, and invasion. *Oncotarget* **7**, 53599–53610, https://doi.org/10.18632/oncotarget.10679 (2016).
48. Kim, C. W. *et al*. ZKSCAN3 Facilitates Liver Metastasis of Colorectal Cancer Associated with CEA-expressing Tumor. *Anticancer research* **36**, 2397–2406 (2016).
49. Lee, S., Cho, Y. E., Kim, J. Y. & Park, J. H. ZKSCAN3 Upregulation and Its Poor Clinical Outcome in Uterine Cervical Cancer. *Int J Mol Sci* **19**, https://doi.org/10.3390/ijms19102859 (2018).
50. Yang, L. *et al*. The previously undescribed ZKSCAN3 (ZNF306) is a novel "driver" of colorectal cancer progression. *Cancer Res* **68**, 4321–4330, https://doi.org/10.1158/0008-5472.CAN-08-0407 (2008).
51. Yang, L. *et al*. Evidence of a role for the novel zinc-finger transcription factor ZKSCAN3 in modulating Cyclin D2 expression in multiple myeloma. *Oncogene* **30**, 1329–1340, https://doi.org/10.1038/onc.2010.515 (2011).
52. Reina-Campos, M., Moscat, J. & Diaz-Meco, M. Metabolism shapes the tumor microenvironment. *Curr Opin Cell Biol* **48**, 47–53, https://doi.org/10.1016/j.ceb.2017.05.006 (2017).
53. Liao, Y., Smyth, G. K. & Shi, W. The Subread aligner: fast, accurate and scalable read mapping by seed-and-vote. *Nucleic Acids Res* **41**, e108, https://doi.org/10.1093/nar/gkt214 (2013).
54. Quinlan, A. R. & Hall, I. M. BEDTools: a flexible suite of utilities for comparing genomic features. *Bioinformatics* **26**, 841–842, https://doi.org/10.1093/bioinformatics/btq033 (2010).
55. Bailey, T. L. *et al*. MEME SUITE: tools for motif discovery and searching. *Nucleic Acids Res* **37**, W202–208, https://doi.org/10.1093/nar/gkp335 (2009).
56. Love, M. I., Huber, W. & Anders, S. Moderated estimation of fold change and dispersion for RNA-seq data with DESeq2. *Genome biology* **15**, 550, https://doi.org/10.1186/s13059-014-0550-8 (2014).
57. Ohler, U., Liao, G. C., Niemann, H. & Rubin, G. M. Computational analysis of core promoters in the Drosophila genome. *Genome biology* **3**, RESEARCH0087 (2002).

Acknowledgements

Author contributions

M.B. performed all experiments for Figures 1, 2, 5, 6 and Figures S1,S3 and RNA and ChIP preparations related to Figures 3–5. M.P. performed high throughput library preparations and sequencing related to Figures 3,4. M.E. performed experiments related to Figure S2. N.C. provided technical assistance. A.S. and M.P. performed bioinformatics analyses related to Figures 3,4,5. Y.G. and A.S. secured financial support. All authors reviewed the manuscript.

Competing interests

The authors declare no competing interests.

Additional information

Supplementary information is available for this paper at https://doi.org/10.1038/s41598-020-66377-z.

Correspondence and requests for materials should be addressed to A.J.S.

Reprints and permissions information is available at www.nature.com/reprints.

Publisher's note Springer Nature remains neutral with regard to jurisdictional claims in published maps and institutional affiliations.